MINIMISATION OF OPERATING CYCLE DURATION AND ENERGY LOSSES IN AN OVERHEAD CRANE TRAVELING MECHANISM

Valentyn Kovalenko[1][0000-0001-9161-198X], Maksym Strelkov[1], Vsevolod Stryzhak[1][0000-0001-9161-198X], Sergey Iglin[1] [0000-0002-9144-7427], Evgen Druzhinin[1][0000-0002-1774-9582], Oleksandr Istomin[1][0000-0002-5709-6459]
[1]National Technical University "Kharkiv Polytechnic Institute", Ukraine
vsevolod.stryzhak@khpi.edu.ua

Abstract - The aim of the study is to develop a comprehensive optimisation criterion that ensures a balance between the duration of the working cycle of the bridge crane movement mechanism and its energy efficiency. To achieve this goal, a mathematical model of the "movement mechanism–metal structure–load" system was developed, taking into account the mechanical characteristics of the electric drive. An analysis of the dynamics was performed, an optimisation problem was formulated, and a comprehensive optimisation criterion was substantiated, ensuring the fulfilment of the final control conditions in the minimum possible time and with minimal energy losses in the electric drive. Optimisation of the movement of the "movement mechanism–metal structure–load" system in accordance with the objective function involves variation of the stages of the working cycle – acceleration, uniform motion, and braking – as well as variation of the load suspension length. Additionally, at the end of the working cycle, a short acceleration and braking stage can be applied to correct the phase of load oscillations in order to eliminate them. The most significant result is the development of a comprehensive optimisation criterion that combines the minimisation of the total duration of the working cycle and the integral energy loss indicator. The peculiarity of this study is that the loss indicator is the root mean square acceleration, which characterises the intensity of the lag of the actual electric motor speed relative to the ideal no-load speed and the corresponding losses in the asynchronous motor. The significance of the obtained results lies in the fact that the proposed method makes it possible to achieve a balance between the duration of the working cycle and energy losses by varying the parameters of the working cycle.

Keywords: Overhead crane, Movement mechanism, Optimisation, Oscillation, Electric drive.

1. Introduction

Research into optimal control is of great interest to researchers. In this field of research, the issue of optimal control of crane systems occupies a significant place. The great relevance of optimising the movement of crane mechanisms is evidenced by the large number of publications on this topic. In particular, many studies have been conducted in recent years.

The problem of controlling a three-dimensional bridge crane as a significantly nonlinear system with partially measured state variables under the conditions of ensuring time-optimal and collision-free movement of load in a space with obstacles has been solved [1]. The set goal is achieved by combining motion planning with consideration of system constraints and the synthesis of a robust second-order controller based on an extended state observer, which provides estimation of unmeasured variables and compensation for disturbances with Lyapunov stability of the closed system. This allows for increased positioning accuracy, reduced influence of external disturbances, and fast crane operation in a complex three-dimensional environment.

The limitations of traditional methods of controlling a three-dimensional bridge crane, which do not provide optimal trajectory planning taking into account dynamic constraints, adequate robustness to uncertainties and disturbances, and guaranteed convergence time of the observer and controller, have been eliminated [2]. The problem of simultaneously ensuring time-optimal motion, effective disturbance suppression, and fixed state estimation time for a nonlinear 3DOC system has been solved. This allows for increased motion accuracy, guaranteed fixed disturbance

dx.doi.org/10.17683/ijomam/issue23.18

compensation time, and significantly improved overall dynamic control quality.

The complexity of controlling and stabilising the oscillations of a double pendulum bridge crane, which is characterised by significant non-linearity and sensitivity to uncertainties and external disturbances, has been overcome [3]. The problem of nonlinear optimal control with guaranteed stability and tracking of specified trajectories for all state variables has been solved in order to ensure fast and accurate tracking of reference values under conditions of moderate variations in control actions and the presence of disturbances.

The problem of reducing the movement time of a bridge crane while simultaneously eliminating residual load oscillations during manoeuvres of the "from rest to rest" type, which is critical for systems with pendulum dynamics and limited drive power, has been solved [4]. The combination of maximum possible use of motor resources with effective vibration suppression in a double pendulum system has been ensured. The method reduces the duration of the manoeuvre by more than 23% compared to the classical approach to crane control.

The problem of ensuring the movement of a bridge crane trolley with a limited load swing angle in conditions of wind disturbances and limited communication and computing resources in the network interaction of several cranes has been solved [5]. Simultaneous achievement of the specified trolley position and compliance with safe load deviation limits have been ensured with reduced use of network and computing resources.

The problem of compromise between speed and energy efficiency during ship loading and unloading operations has been solved, taking into account restrictions on container height and energy consumption and recovery processes [6]. This task has been formalised as optimal control with correct consideration of obstacle avoidance constraints and drive energy characteristics, which significantly reduces energy consumption while maintaining a virtually unchanged loading and unloading cycle duration.

The task of improving the energy efficiency of bridge crane control during repeated manoeuvres of the "from rest to rest" type with simultaneous elimination of residual load oscillations has been solved [7]. A reduction in energy consumption has been achieved without compromising the dynamic quality of movement and operational safety. This has been achieved by modifying the smoothed single-mode command generator with the introduction of an additional constant and its optimisation based on a linearised motion model, as well as by using the possibility of varying the duration of the manoeuvre to achieve minimum energy consumption.

The modification of control constraints in the problem of time-optimal control of a simple pendulum with a moving suspension point is justified, which allows revising the classical formulation of the problem and expanding the admissible region of control actions [8]. Time optimisation problems for classical and modified constraints are formulated and compared by analytically integrating the equations of motion, followed by reducing the problem to a constrained nonlinear programming problem and its numerical solution using the particle swarm method. The proposed solutions have been experimentally tested [9].

The problem of suppressing simultaneous oscillations of a suspended container and liquid splashing during load transportation by a bridge crane has been solved, taking into account restrictions on controllable and uncontrollable states, as well as requirements for movement time and energy consumption [10]. The formalisation of a complex pendulum-hydrodynamic system within the limits of optimal trajectory planning has been ensured.

The problem of suppressing the swaying of the load of a bridge crane in the presence of wind disturbances and variable rope length has been solved, while ensuring that the trolley reaches the specified position within a limited time [11]. The processes of lifting or lowering the load have been coordinated with the requirement to minimise the angle of deviation during movement.

The problem of suppressing swaying and ensuring the specified transition characteristics of a bridge crane with a double spherical pendulum and variable rope length during the simultaneous movement of the trolley, bridge and lifting/lowering of the load has been solved [12]. Correct consideration of nonlinear relationships and dynamics without simplifying the model has been ensured, allowing minimisation of transport time while guaranteeing full compliance with all system constraints.

The positioning of the bridge crane load with three degrees of freedom has been developed with minimisation of swaying and improvement of transient characteristics to increase operational safety [13]. Simultaneous improvement of control quality and the possibility of safe navigation in a complex environment have been ensured by applying an integral LQR controller with weight matrix optimisation using the differential evolution method and using a modified local path planning algorithm to form a rational motion trajectory.

Optimising crane systems requires, first and foremost, the creation of a mathematical model, which is characteristic of both jib cranes [14] and bridge cranes [15], as shown in the examples of complex crane systems. Three-dimensional process modelling can be used [16]. After that, in accordance with optimisation methods, the objective function and the initial and final conditions are justified.

This study uses the Sequential Quadratic Programming (SQP) algorithm, which is a primary method for solving constrained nonlinear optimisation problems [17] and is highly regarded for its efficiency and fast convergence rate.

Thus, a review of the current state of research shows that the areas of optimal working cycle duration and control energy consumption are currently at the forefront of scientific work in the field of crane motion optimisation. However, the question of the balance between these two components of efficiency improvement remains almost unexplored. In particular, studies on crane movement optimisation hardly take into account the characteristics of the electric drive and its control modes, which is considered in this study.

2. Mathematical Model of the "Movement Mechanism-metal Structure-load" System

Let us examine the interaction between the crane and the frequency-controlled drive. To do this, we will represent the crane as a model of the "movement mechanism-metal structure-load" system The calculation diagram of this system is shown in Fig. 1.

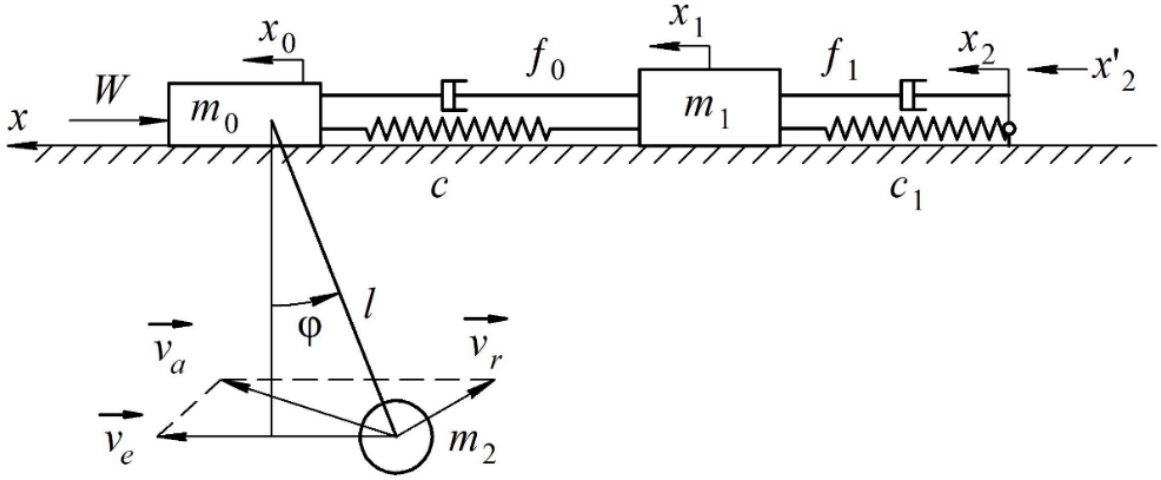

m_1 – the mass of the electric motor and the rotating masses of the drive on the first shaft; m_0 – the mass of the parts of the crane that move in a translational manner; m_2 – mass of the load; f_0 and f_1 – damping coefficients of the transmission mechanism shafts and the output shaft of the movement mechanism, respectively; c and c_1 – reduced stiffness of the transmission mechanism and the output shaft of the movement mechanism, respectively; v_e – transfer speed of the load; v_r – relative speed of the load; v_a – absolute speed of the load; W – static resistance force of movement per drive; l – load suspension length; x_2 – displacement of the system's input point, reduced to the translational motion of the crane; $\dot{x}_2$ – speed of the system's input point (electric motor speed), reduced to the translational motion of the crane; x_1 – mass displacement m_1; x_0 – mass displacement m_0; φ – angle of deviation of the load from the vertical

Figure 1: Calculated 3-mass dynamic diagram of the "movement mechanism-metal structure-load" system

When developing the mathematical model, a number of assumptions were made:

– the mass of the bridge structure and the equipment mounted on it is assumed to be uniformly distributed along the entire length of the bridge.

– the moments of inertia of the main and end beams are assumed to be constant along the lengths of the corresponding elements of the metal structure.

– the crane bridge is symmetrically loaded, with the load trolley positioned at the mid-span; the drive wheels have identical diameters, are installed without skew, and the crane moves without longitudinal or transverse wheel slippage relative to the crane track.

Let us formulate the equations of motion for this mechanical system.

The kinetic energy of the system is given by:

$$T = T_1 + T_0 + T_2 \tag{1}$$

where the kinetic energies of the corresponding masses are:

$$T_1 = \frac{m_1 \dot{x}_1^2}{2}, T_0 = \frac{m_0 \dot{x}_0^2}{2}, T_2 = \frac{m_2 v_a^2}{2}, \tag{2}$$

To calculate the kinetic energy of the load's movement, it is necessary to determine its absolute speed:

$$v_a^2 = v_e^2 + v_r^2 + 2 \cdot v_e \cdot v_r \cdot \cos(180° - \varphi) = \\ = \dot{x}_0^2 + l^2 \cdot \dot{\varphi}^2 - 2 \cdot \dot{x}_0 \cdot l \cdot \dot{\varphi} \cdot \cos\varphi \quad (3)$$

The potential energy of the system:

$$V = -m_2 \cdot g \cdot l \cdot \cos\varphi + \\ + \frac{c}{2}(x_1 - x_0)^2 + \frac{c_1}{2}(x_2 - x_1)^2, \quad (4)$$

Relay function (dissipation energy):

$$\Phi = \frac{f_0}{2}(\dot{x}_1 - \dot{x}_0)^2 + \frac{f_1}{2} \cdot \dot{x}_1^2 \quad (5)$$

Let us write down the Lagrange equation for this system:

$$\begin{cases} \frac{d}{dt}\left(\frac{\partial T}{\partial \dot{x}_1}\right) - \frac{\partial T}{\partial x_1} = Q_{x_1} \\ \frac{d}{dt}\left(\frac{\partial T}{\partial \dot{x}_0}\right) - \frac{\partial T}{\partial x_0} = Q_{x_0} \\ \frac{d}{dt}\left(\frac{\partial T}{\partial \dot{\varphi}}\right) - \frac{\partial T}{\partial \varphi} = Q_{\varphi} \end{cases} \quad (6)$$

where:

$$Q_{x_1} = -\frac{\partial V}{\partial x_1} - \frac{\partial \Phi}{\partial \dot{x}_1} \\ Q_{x_0} = -\frac{\partial V}{\partial x_0} - W \cdot \operatorname{sign}\dot{x}_0 \quad (7) \\ Q_{\varphi} = -\frac{\partial V}{\partial \varphi} - \frac{\partial \Phi}{\partial \dot{\varphi}}$$

According to (6), we will form the equation for the mechanism under consideration

$$\frac{\partial T}{\partial \dot{x}_1} = m_1 \cdot \dot{x}_1 \\ \frac{\partial T}{\partial \dot{x}_0} = m_0 \cdot \dot{x}_0 - m_2 \cdot \cos\varphi \cdot l \cdot \dot{\varphi} + m_2 \cdot \dot{x}_0 = \\ = (m_0 + m_2) \cdot \dot{x}_0 - m_2 \cdot \cos\varphi \cdot l \cdot \dot{\varphi} \quad (8) \\ \frac{\partial T}{\partial \dot{x}_0} = m_0 \cdot \dot{x}_0 - m_2 \cdot \cos\varphi \cdot l \cdot \dot{\varphi} + m_2 \cdot \dot{x}_0 = \\ = (m_0 + m_2) \cdot \dot{x}_0 - m_2 \cdot \cos\varphi \cdot l \cdot \dot{\varphi}$$

$$\frac{d}{dt}\left(\frac{\partial T}{\partial \dot{x}_1}\right) = m_1 \cdot \ddot{x}_1 \\ \frac{d}{dt}\left(\frac{\partial T}{\partial \dot{x}_0}\right) = (m_0 + m_2) \cdot \ddot{x}_0 - \\ - m_2 \cdot l \cdot (\cos\varphi \cdot \ddot{\varphi} - \sin\varphi \cdot \dot{\varphi}^2) \quad (9) \\ \frac{d}{dt}\left(\frac{\partial T}{\partial \dot{\varphi}}\right) = m_2 \cdot l \cdot \left[l \cdot \ddot{\varphi} - \begin{pmatrix} \ddot{x}_0 \cdot \cos\varphi - \\ -\dot{x}_0 \cdot \sin\varphi \cdot \dot{\varphi} \end{pmatrix} \right] = \\ = m_2 \cdot l \cdot (l \cdot \ddot{\varphi} - \ddot{x}_0 \cdot \cos\varphi + \dot{x}_0 \cdot \sin\varphi \cdot \dot{\varphi});$$

$$\frac{\partial T}{\partial x_1} = \frac{\partial T}{\partial x_0} = 0 \\ \frac{\partial T}{\partial \varphi} = m_2 \cdot \dot{x}_0 \cdot l \cdot \dot{\varphi} \cdot \sin\varphi \quad (10)$$

$$\frac{\partial V}{\partial x_1} = c \cdot (x_1 - x_0) - c_1 \cdot (x_2 - x_1) \\ \frac{\partial \Pi}{\partial x_0} = -c \cdot (x_1 - x_0) \quad (11) \\ \frac{\partial \Pi}{\partial \varphi} = m_2 \cdot g \cdot l \cdot \sin\varphi$$

$$\frac{\partial \Phi}{\partial \dot{x}_1} = f_0 \cdot (\dot{x}_1 - \dot{x}_0) + f_1 \cdot \dot{x}_1 \\ \frac{\partial \Phi}{\partial \dot{x}_0} = -f_0 \cdot (\dot{x}_1 - \dot{x}_0) \quad (12) \\ \frac{\partial \Phi}{\partial \dot{\varphi}} = 0$$

Taking into account the above transformations, we obtain a system of equations:

$$\begin{cases} m_1 \cdot \ddot{x}_1 = -c \cdot (x_1 - x_0) + \\ \quad + c_1 \cdot (x_2 - x_1) - f_0 \cdot (\dot{x}_1 - \dot{x}_0) - f_1 \cdot \dot{x}_1 \\ (m_0 + m_2) \cdot \ddot{x}_0 - m_2 \cdot l \cdot (\cos\varphi \cdot \ddot{\varphi} - \sin\varphi \cdot \dot{\varphi}^2) = \\ \quad = c \cdot (x_1 - x_0) + f_0 \cdot (\dot{x}_1 - \dot{x}_0) - W \cdot \operatorname{sign}\dot{x}_0 \\ m_2 \cdot l \cdot (l \cdot \ddot{\varphi} - \ddot{x}_0 \cdot \cos\varphi + \dot{x}_0 \cdot \sin\varphi \cdot \dot{\varphi}) - \\ \quad - m_2 \cdot \dot{x}_0 \cdot l \cdot \dot{\varphi} \cdot \sin\varphi = -m_2 \cdot g \cdot l \cdot \sin\varphi \end{cases} \quad (13)$$

After elementary transformations, we obtain:

$$\begin{cases} m_1 \cdot \ddot{x}_1 + f_1 \cdot \dot{x}_1 + f_0 \cdot (\dot{x}_1 - \dot{x}_0) + \\ \quad + c \cdot (x_1 - x_0) - c_1 \cdot (x_2 - x_1) = 0 \\ (m_0 + m_2) \cdot \ddot{x}_0 - m_2 \cdot l \cdot \cos\varphi \cdot \ddot{\varphi} + \\ \quad + m_2 \cdot l \cdot \sin\varphi \cdot \dot{\varphi}^2 - f_0 \cdot (\dot{x}_1 - \dot{x}_0) - \\ \quad - c \cdot (x_1 - x_0) = -W \cdot \mathrm{sign}\dot{x}_0 \\ l \cdot \ddot{\varphi} - \ddot{x}_0 \cdot \cos\varphi + g \cdot \sin\varphi = 0 \end{cases} \quad (14)$$

Let us link the resulting system of equations of motion of the model with the equation of motion of the electric drive. Since the equation of motion of the electric drive has the form:

$$T_{\text{м}} \cdot \frac{d\omega}{dt} + \omega = \omega_0 - \frac{M_{\text{st}}}{\beta}; \quad (15)$$

where: $M_{\text{ст}}$ – total static torque reduced to the electric motor shaft

J_Σ is the total moment of inertia reduced to the electric motor shaft

ω is the current angular velocity of the drive electric motor

ω_0 is the current ideal no-load speed of the drive electric motor

$$\omega_0 = \frac{2\pi}{p} f \quad (16)$$

p – number of pole pairs of the drive electric motor

f – supply voltage frequency

$T_{\text{м}}$ – electromechanical time constant;

$$T_{\text{м}} = J_\Sigma / \beta \quad (17)$$

β – stiffness of the mechanical characteristics of the drive motor

The rotational motion of the electric motor can be reduced to the translational motion of the crane through the gear ratio and the wheel radius, which can ultimately be denoted by the coefficient α . Then the motion of point A (Fig. 1) can be expressed taking into account the motion equation of the drive:

$$x_2 = \alpha \left(\frac{2\pi f}{p} - \frac{\alpha M_{\text{ст}}}{\beta} - \frac{J_\Sigma}{\beta} \dot{\omega} \right) \quad (18)$$

For a numerical solution, the system of differential equations (14) must be reduced to the form:

$$M(t, \vec{y}) d\vec{y}/dt = \vec{F}(t, \vec{y}) \quad (19)$$

where: M is the mass matrix;

$\vec{y}$ is the column vector of variables;

$\vec{F}$ is the column vector of functions. Each component of this vector is a function of the argument t and the coordinates of the vector $\vec{y}$.

The initial condition for this system is: $\vec{y}(0) = \vec{y}_0$ (each coordinate of the vector $\vec{y}$ is specified).

Let us introduce the variables:

$$\begin{aligned} &y_1 = x_1;\ y_2 = \dot{x}_1;\ y_3 = x_0; \\ &y_4 = \dot{x}_0;\ y_5 = \varphi;\ y_6 = \dot{\varphi}; \end{aligned} \quad (20)$$

Then the system of equations will be written as follows:

$$\begin{cases} \dot{y}_1 = y_2; \\ m_1 \dot{y}_2 = -f_1 \cdot y_2 - f_0 (y_2 - y_4) - \\ \quad - c(y_1 - y_3) + c_1 (x_2(t) - y_1) = 0 \\ \dot{y}_3 = y_4 \\ (m_0 + m_2) \dot{y}_4 - m_2 l \cos y_5 \dot{y}_5 \dot{y}_6 \\ \quad = -m_2 l \sin y_5 y_6^2 + f_0 \cdot (y_2 - y_4) \\ \quad + c \cdot (y_1 - y_3) - W \cdot \mathrm{sign}(y_4) \\ \dot{y}_5 = y_6 \\ l\dot{y}_6 - \cos(y_5) \dot{y}_4 = -g \cdot \sin y_5 \end{cases} \quad (21)$$

We reduce it to the form (19):

$$\vec{y} = \begin{pmatrix} y_1 \\ y_2 \\ y_3 \\ y_4 \\ y_5 \\ y_6 \end{pmatrix}; M(t, \vec{y}) = \begin{pmatrix} 1 & 0 & 0 & 0 & 0 & 0 \\ 0 & m_1 & 0 & 0 & 0 & 0 \\ 0 & 0 & 1 & 0 & 0 & 0 \\ 0 & 0 & 0 & m_0 + m_2 & 0 & -m_2 l \cos(y_5) \\ 0 & 0 & 0 & 0 & 1 & 0 \\ 0 & 0 & 0 & -\cos(y_5) & 0 & l \end{pmatrix} \quad (22)$$

$$\vec{F}(t, \vec{y}) = \begin{pmatrix} y_2 \\ -f_1 y_2 - f_0 (y_2 - y_4) - \\ \quad - c(y_1 - y_3) - c_1 y_1 + c_1 x_2(t) \\ y_4 \\ -m_2 l \sin(y_5) y_6^2 + f_0 (y_2 - y_4) + \\ \quad + c(y_1 - y_3) - W \mathrm{sign}(y_4) \\ y_6 \\ -g \sin(y_5) \end{pmatrix} \quad (23)$$

3. Analysis of Dynamics

Four modes of change in the supply voltage frequency of an electric motor during start-up and braking are considered:

-linear:

$$f(t)=\begin{cases}\dfrac{f_{\max}}{t_a}\cdot t; & t\le t_a\\ f_{\max}; & t>t_a\end{cases} \quad (24)$$

- quadratic:

$$f(t)=\begin{cases}f_{\max}-\dfrac{f_{\max}(t-t_a)^2}{t_a^2}\cdot t; & t\le t_a\\ f_{\max}; & t>t_a\end{cases} \quad (25)$$

- cubic:

$$f(t)=\begin{cases}\dfrac{f_{\max}\cdot t^2}{t_a^3}(3t_a-2t); & t\le t_a\\ f_{\max}; & t>t_a\end{cases} \quad (26)$$

– trigonometric:

$$f(t)=\begin{cases}\dfrac{f_{\max}\cdot t}{t_a}-\dfrac{f_{\max}}{2\pi}\sin\dfrac{2\pi\cdot t}{t_a}; & t\le t_a\\ f_{\max}; & t>t_a\end{cases} \quad (27)$$

The parameters of the crane for which the calculation is performed are given in Table 1.

Table 1. Summarises the system parameters used in modelling

No	Parameter name	Designation, dimension	Value
1	Reduced mass of the electric motor and rotating masses of the drive on the first shaft	m_1, kg	786.5
2	Mass of the parts of the crane that move in a translational manner	m_0, kg	21680
3	Weight of load	m_2, kg	15000
4	Damping coefficient of transmission mechanism shafts	f_0, kg/s	$2.23\cdot10^5$
5	Damping coefficient of the output shaft of the drive mechanism	f_1, kg/s	0
6	Reduced stiffness of the transmission mechanism	c, N/m	$2.36\cdot10^6$
7	Reduced stiffness of the output shaft of the drive mechanism	c_1, N/m	$3.35\cdot10^6$
8	Static resistance force of the drive per drive	W, N	3234
9	Length of load suspension	l, m	4.5
10	Target coordinates	x_{2f}, m	12

Modelling of the dynamics of the "movement mechanism-metal structure-load" system was performed by numerical integration using equations (21). Using numerical modelling, we will determine the dynamic characteristics of the system's movement under given control laws, which will allow us to evaluate the mathematical model and determine the behaviour of the system under normal control. The graphs of the change in the dynamic characteristics of motion are shown in Fig. 2, and the motion of the point in phase coordinates is shown in Fig. 3.

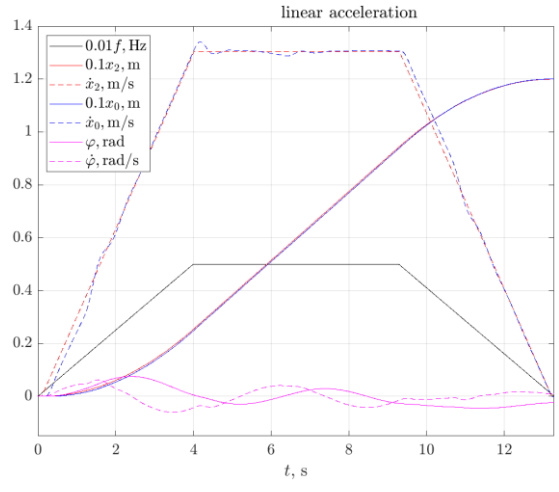

a

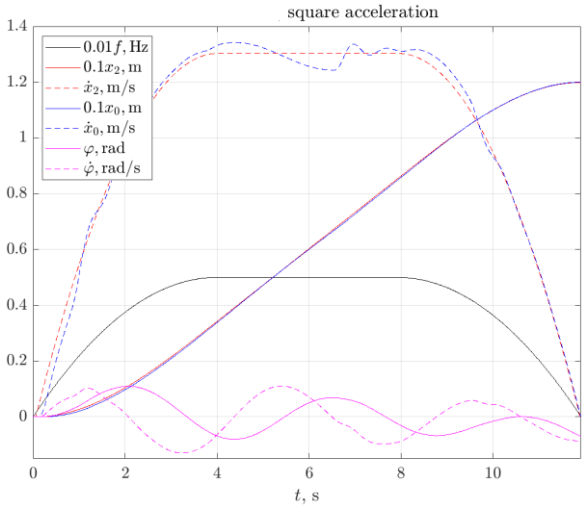

b

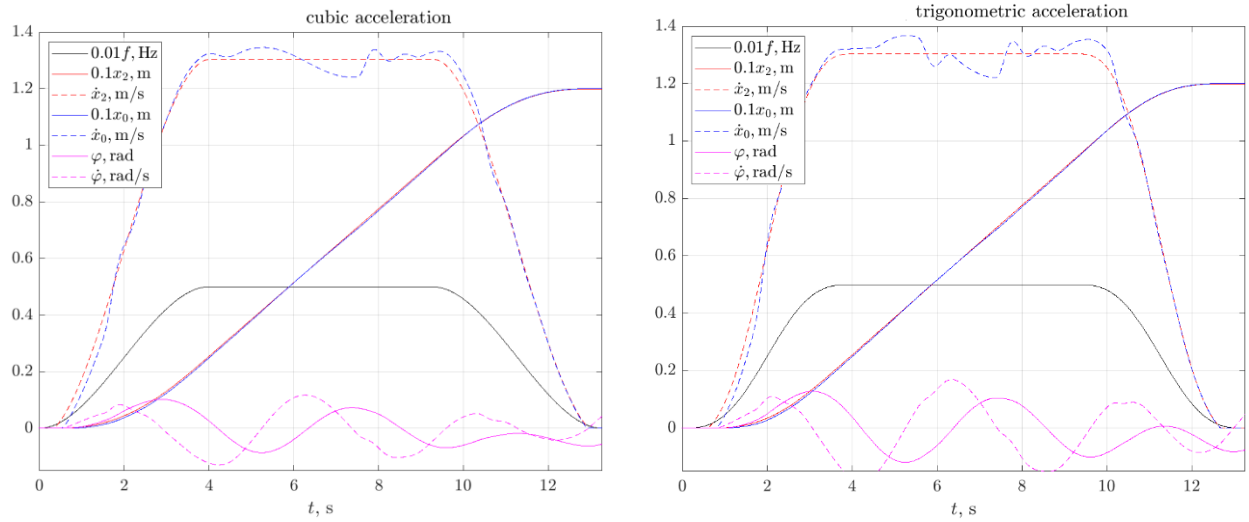

c d

modes of changing the frequency of the electric motor supply voltage: a – linear, b – quadratic; c – cubic; d – trigonometric

Figure 2: Analysis of the dynamics of the "movement mechanism-metal structure-load" system

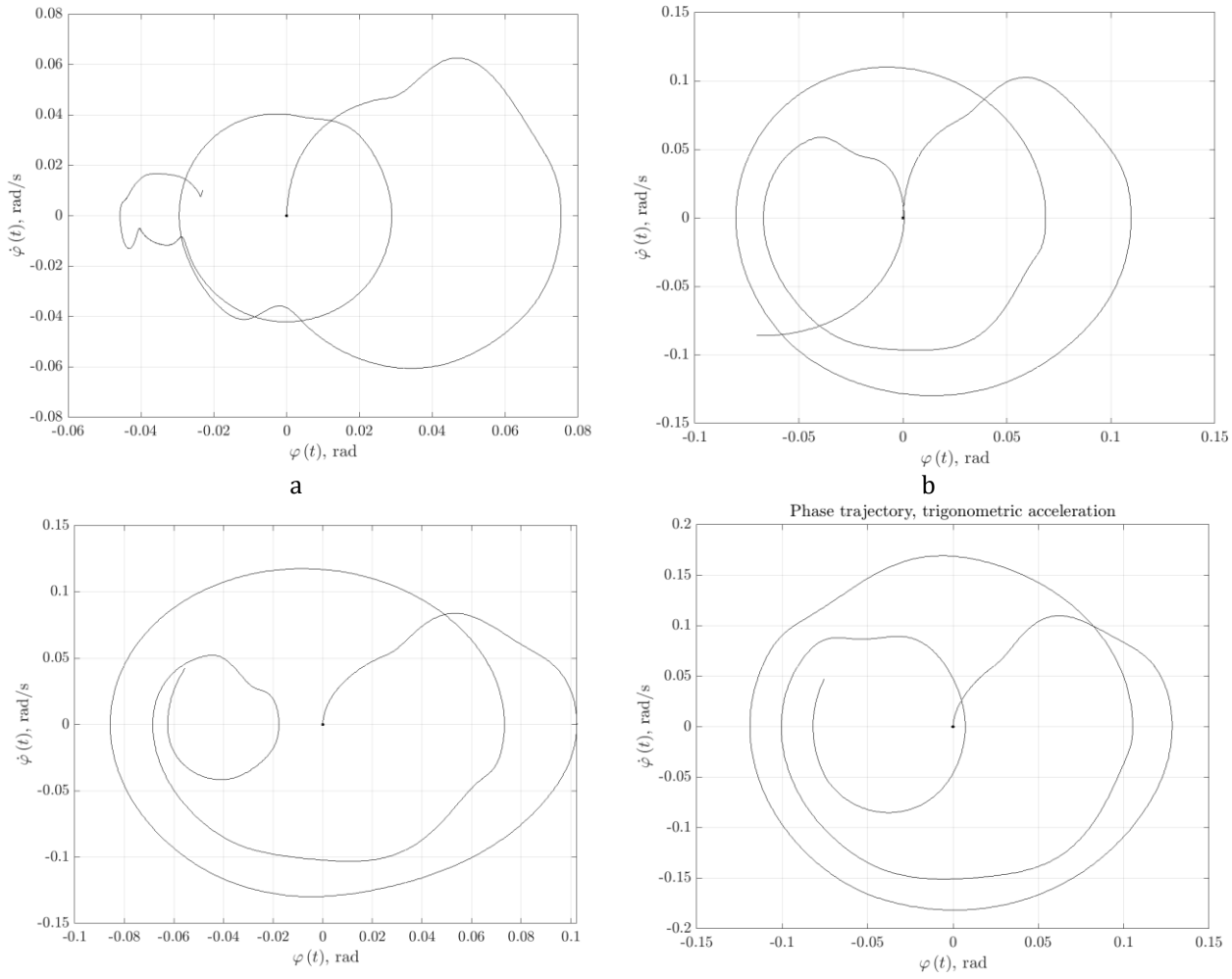

a b

c d

modes of changing the frequency of the electric motor supply voltage: a – linear, b – quadratic; c – cubic; d – trigonometric

Figure 3: Phase trajectories of load movement in the analysis of the dynamics of the "movement mechanism-metal structure-load" system

4. Movement Optimisation

Based on the research objective, the task of optimising the "movement mechanism-metal structure-load" system was formulated: to move the system from its initial state with zero coordinates to its final state at a given distance with minimum deviation angle and angular velocity of the load in minimum time and with minimum energy consumption.

To find the solution, the form of change in the supply current frequency of the working cycle of the movement mechanism was determined, the diagram of which is shown in Fig. 4 using the example of a quadratic acceleration and deceleration mode.

This graph of the optimal movement of the travel mechanism has an almost standard shape, consisting of acceleration, uniform motion and braking, but differs in that it has an additional start-braking phase. An additional start-braking stage may occur before a complete stop. Its task is to correct the phase for more effective elimination of load oscillation and bringing the system closer to the desired final state.

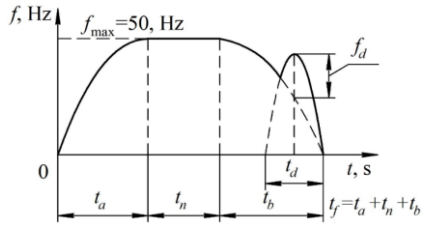

t_a t_n – acceleration duration; t_b – uniform motion duration; t_d – braking duration; – additional start-braking stage duration; $f_{\max}$ – maximum motor supply current frequency throughout the entire working cycle; f_d – maximum motor supply current frequency during the additional start-braking stage

Figure 4: Diagram of the change in the frequency of the electric motor supply during the working cycle of the bridge crane's movement mechanism to find the optimal solution

From the system of equations (21) and the diagram in Fig. 4, we determine the parameters that can be varied to find the law of optimal motion and introduce the following designations for them:

- acceleration duration $b_1 = t_a$;
- duration of uniform motion $b_2 = t_n$;
- braking duration $b_3 = t_b$;
- duration of additional braking $b_4 = t_d$;
- maximum frequency of the motor supply current during the additional start-braking stage $b_5 = f_d$;
- the length of the load suspension $b_6 = l$.

For variable parameters, restrictions are introduced that form the framework of the real crane for the variable parameters. For the crane under study, these restrictions are:

acceleration and braking duration. Since control is set kinematically, through speed, the restriction on the driving force is determined by the minimum acceleration and braking duration, which cannot be less than the minimum value (in practice, this would mean overload of the drive motor with subsequent wheel slip). In addition, the upper limit of the duration of the start-braking processes also needs to be limited, since their excessive duration leads to a decrease in the overall efficiency of the crane in practice.

$$3,5 \le b_1 \le 5 \text{ s}; \; 3,5 \le b_3 \le 5 \text{ s} \tag{28}$$

duration of uniform travel

$$0 \le b_2 \le 10 \text{ s} \tag{29}$$

the duration of additional braking cannot exceed the duration of the main braking, but can be zero

$$0 \le b_4 \le b_3 \text{ s} \tag{30}$$

the maximum frequency of the motor supply current during the additional start-braking stage ranges from zero – in the absence of additional start-braking – to the nominal frequency of the steady-state current.

$$0 \le b_5 \le f_{\max} = 50 \text{ Hz} \tag{31}$$

the length of the load suspension varies as an additional factor that allows influencing the oscillation period.

$$2,5 \le b_6 \le 6,5 \text{ m} \tag{32}$$

The objective function is formed from the optimisation aim:

– energy efficiency. This parameter is considered in terms of losses in the electric motor during start-braking processes. The modes of changing the supply frequency of the electric motor set the synchronous speed of the motor, however, as can be seen from equation (18), the actual speed of the rotor lags behind it, forming a slip, which determines the main part of energy losses. Thus, to reduce energy losses, we minimise the value of the root mean square angular acceleration of the motor throughout the entire duration of the mechanism's operating cycle:

$$E_{sl} = \sqrt{\frac{1}{t_f}\int_0^{t_f} \dot{\omega}_0^2(t)\,dt} \to \min \qquad (33)$$

– reduction of the working cycle duration. From the previous optimisation goal, it follows that the best motion law should provide for the longest possible start-braking modes. This can lead to an excessively long working cycle of the mechanism and an increase in the root mean square value of energy consumption. Therefore, it is advisable to introduce an optimisation criterion that will minimise the total working cycle time

$$t_f \to \min \qquad (34)$$

of bringing the system to its final state. In accordance with the control objective, the system has the following initial and final conditions that must be achieved:

$$\begin{gathered} x_0(0)=0;\ \dot{x}_0(0)=0;\ x_0(t_f)=12;\ \dot{x}_0(t_f)=0; \\ \varphi(0)=0;\ \dot{\varphi}(0)=0;\ \varphi(t_f)=0;\ \dot{\varphi}(t_f)=0; \end{gathered} \qquad (35)$$

After adding the final conditions to the conditions for minimising energy losses and the duration of the operating cycle, the objective function takes the form:

$$\begin{gathered} y = W_1\left|x_0(t_f)-x_{2f}\right| + \\ +W_2\left|\dot{x}_0(t_f)\right| + W_3\left|\varphi(t_f)\right| + \\ +W_4\left|\dot{\varphi}(t_f)\right| + W_5 t_f + W_6 E_{sl} \end{gathered} \qquad (36)$$

where: $W_1,\ W_2,\ W_3,\ W_4,\ W_5,\ W_6$ – weight coefficients of the objective function.

The optimisation result is shown in Fig. 5, and the phase trajectories of the load movement are shown in Fig. 6.

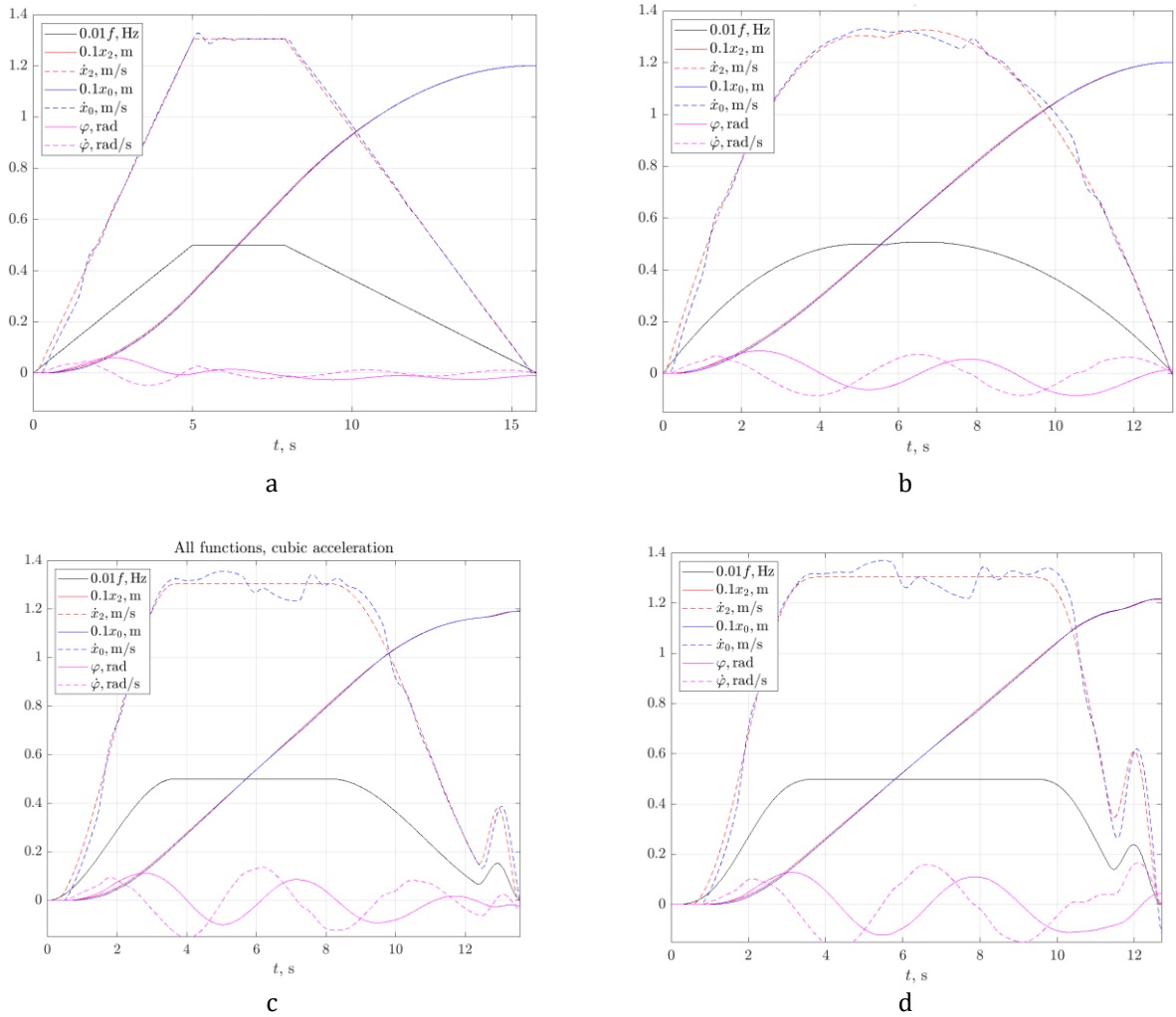

modes of changing the frequency of the electric motor supply voltage: a – linear, b – quadratic; c – cubic; d – trigonometric

Figure 5: Optimised movement of the "movement mechanism-metal structure-load" system

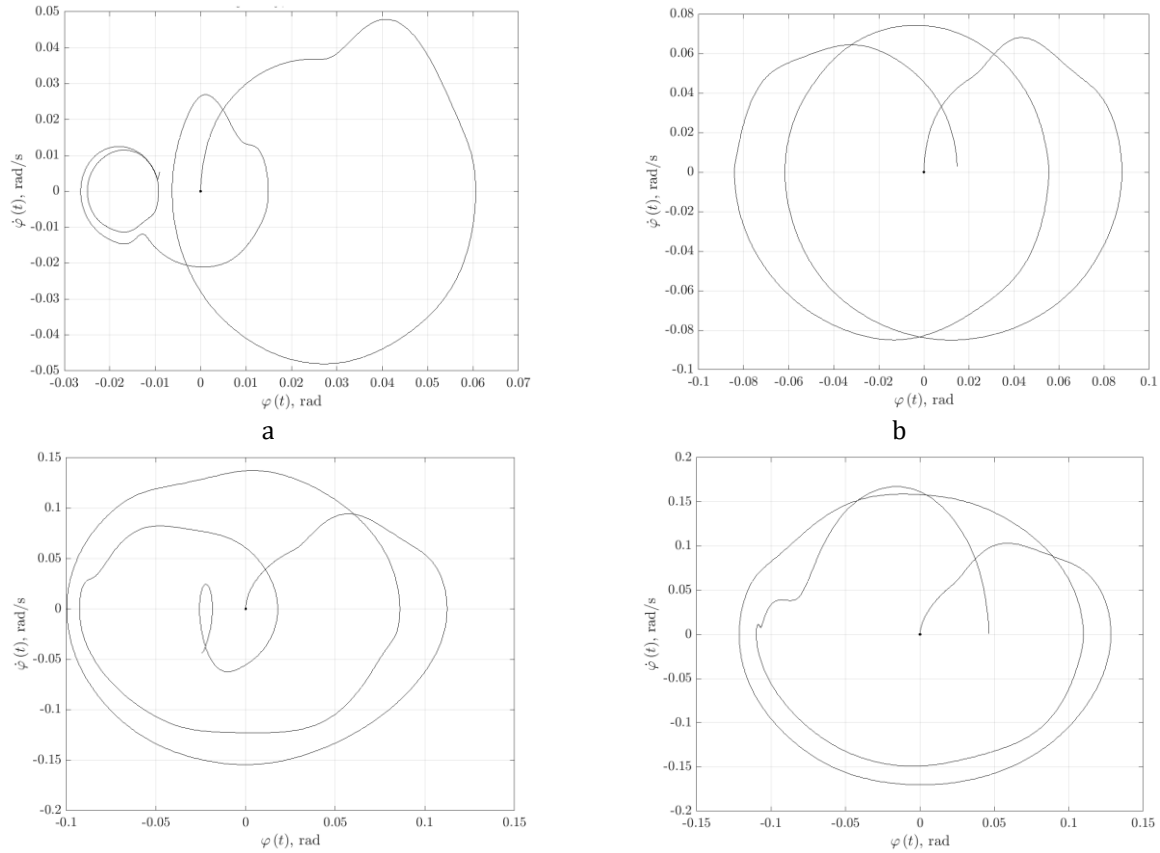

modes of changing the frequency of the electric motor supply voltage: a – linear, b – quadratic; c – cubic; d – trigonometric

Figure 6. Phase trajectories of the optimised movement of the load in the "movement mechanism-metal structure-load" system

5. Discussion

The article provides a solution to the optimisation problem based on a comprehensive criterion of speed and energy loss, which brings the crane system to a given position while eliminating load oscillations. At the first stage of the study, the mechanical system "travel mechanism-metal structure-load" was considered, for which a system of equations describing its motion was compiled. In this part of the study, an analysis of the dynamics under traditional control was performed. The graphs in Fig. 2 show the traditional working cycle of the bridge crane's movement mechanism, in which the acceleration time is equal to the braking time $t_a = t_b = 4$ s . In this case, the crane moves a distance that is selected as the average distance of a typical reloading cycle for a crane with these parameters and is $L_c = 12$ m . The graphs show both the angle of deviation of the load and its angular velocity, which gives an understanding of the nature of the oscillations at the end of the working cycle when both the angle of deviation and its derivative with respect to time must approach zero. Fig. 3 shows that under normal control, at the end of the reloading cycle, there are load oscillations that must be eliminated, which will affect the overall duration of the working cycle of the mechanism and energy consumption.

The obtained mathematical model of the motion of the "movement mechanism-metal structure-load" system is used to solve the optimisation problem. The dynamic characteristics in the optimised working cycle are shown in the graph in Fig. 5. The duration of the acceleration stages may vary compared to normal control in the upward direction (for linear mode it is $t_a = 4,99$ s , for quadratic mode it is $t_a = 4,1$ s) and in the downward direction (for cubic mode it is $t_a = 3,64$ s , for trigonometric mode it is $t_a = 3,85$ s). The braking stage can also be extended within the specified conditions and is as follows for linear mode - $t_b = 7,9$ s , for quadratic mode - $t_b = 7,99$ s , for cubic mode - $t_b = 6,71$ s , for trigonometric mode - $t_b = 4,75$ s .

At the same time, as can be seen from the graphs in Figures 5.c and 5.d, an additional start-braking stage may occur during the general braking stage in order to correct the phase of load oscillations and more accurately fulfil the final control conditions. The total duration of the working cycle increases within the range of 0.24-2.5 s (1.98%-18.85%),

reducing the root mean square acceleration and corresponding energy losses. At the same time, optimal control reduces load oscillations. Fig. 7 shows the scatter field of the end points of the load trajectory on the phase plane for traditional and optimal control.

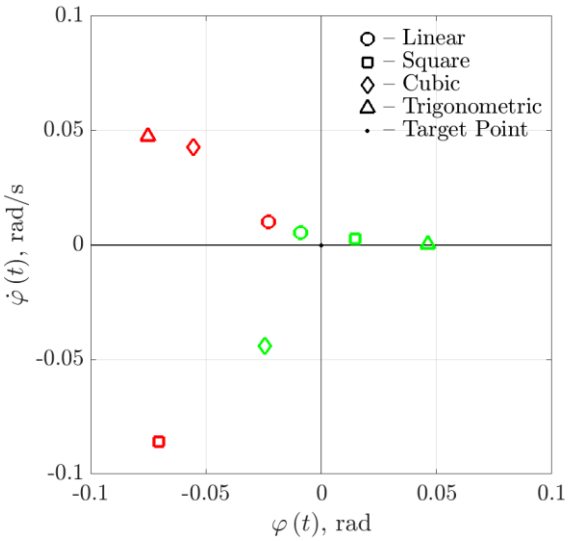

Figure 7: Location of the end points of the load movement trajectory on the phase plane for traditional (red) and optimal control (green) for four modes of changing the supply voltage frequency of the electric motor

Fig. 7 shows that when searching for optimal motion laws, load oscillations are significantly reduced. The effectiveness of reducing oscillations can be assessed in Figure 8, which compares the distance from the end points of the load motion trajectory on the phase plane to the target point of complete rest under traditional and optimal oscillations.

Figure 8 shows a significant reduction in residual load vibrations during optimal operation in all four modes of electric motor supply voltage frequency variation. The graph shows that the best solution is the linear and quadratic modes, while the cubic and trigonometric modes produce large residual vibrations, even when using an additional start-braking stage.

Unlike the articles cited in the literature review, this study takes into account both the reduction in the duration of the working cycle and the energy efficiency of the movement mechanism. The closest is the study [6], which proposes a comprehensive optimisation of speed and energy consumption. However, the approach proposed in this study is aimed not at reducing energy consumption, but at minimising losses in the motor. The disadvantage of this study is the lack of a final elimination of oscillations, which may be the subject of further research.

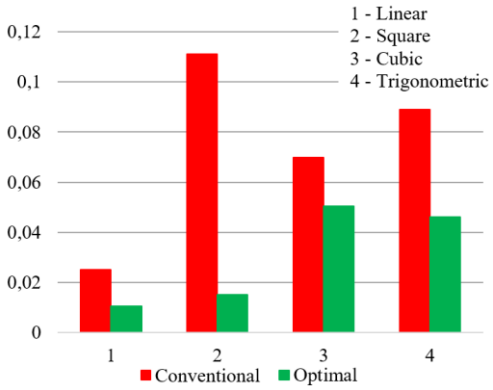

Figure 8: Distance to the target point (complete elimination of oscillations) of the phase trajectory of the load movement with traditional and optimal control for four modes of changing the supply voltage frequency of the electric motor

6. Conclusions

The study has developed a comprehensive optimisation criterion that ensures a balance between the duration of the working cycle of the bridge crane's movement mechanism and its energy efficiency. A mathematical model of the "movement mechanism-metal structure-load" system has been developed, taking into account the mechanical characteristics of the electric drive, an analysis of the dynamics was performed, an optimisation task was formulated, and a comprehensive optimisation criterion was substantiated, which ensures the fulfilment of the final control conditions in the minimum possible time and with minimal energy losses in the electric drive. The movement of the system was modelled under traditional and optimised control.

References

[1] Nguyen, V. C., Thi, H. L., Khanh, H. B. T., Danh, H. N., Duc, D. P., & Nguyen, T. L. (2024). An integrated solution for 3D overhead cranes: Time-optimal motion planning, obstacle avoidance, and anti-swing. *Engineering Science and Technology, an International Journal*, *59*. https://doi.org/10.1016/j.jestch.2024.101852

[2] Chung Nguyen, V., Luu Thi, H., Bui Thi Khanh, H., Huy Nguyen, D., Vu, M. N., & Lam Nguyen, T. (2025). Flatness-Based Motion Planning and Control Strategy of a 3D Overhead Crane. *IEEE Access*, *13*. https://doi.org/10.1109/ACCESS.2024.3524404

[3] Rigatos, G. (2024). Nonlinear Optimal Control for the Underactuated Double-Pendulum Overhead Crane. *Journal of Vibration Engineering and Technologies*, *12*(2). https://doi.org/10.1007/s42417-023-00902-y

[4] Majeed, M. A., Alali, M., Alghanim, K., & Alfadhli, A. (2025). Integrated time-optimal rigid-body and zero-vibration shapers on a two degrees of freedom overhead crane system. *JVC/Journal of Vibration and Control*, *31*(11–12). https://doi.org/10.1177/10775463241257743

[5] Wang, J., Tian, Z., Sun, J., Yang, J., & Li, S. (2025). Event-Triggered Safety-Critical Model Predictive Control for Underactuated Overhead Cranes. *IEEE Transactions on Industrial Informatics*, *21*(9). https://doi.org/10.1109/TII.2025.3567405

[6] Barbosa, F. M., Kullberg, A., & Löfberg, J. (2023). Fast or Cheap: Time and Energy Optimal Control of Ship-to-Shore Cranes. *IFAC-PapersOnLine*, *56*(2). https://doi.org/10.1016/j.ifacol.2023.10.1445

[7] Alhazza, K. A. (2026). Energy Efficient Control of an Overhead Crane by Optimising a Smooth Waveform Command Shaper. *Journal of Vibration and Acoustics*, *148*(2). https://doi.org/10.1115/1.4070069

[8] Loveikin, V. S., Romasevich, Y. A., Khoroshun, A. S., & Shevchuk, A. G. (2018). Time-Optimal Control of a Simple Pendulum with a Movable Pivot. Part 1. *International Applied Mechanics*, *54*(3). https://doi.org/10.1007/s10778-018-0887-x

[9] Loveikin, V. S., Romasevich, Y. A., Khoroshun, A. S., & Shevchuk, A. G. (2020). Time-optimal Control of a Simple Pendulum with a Movable Pivot. Part 2. *International Applied Mechanics*, *56*(2). https://doi.org/10.1007/s10778-020-01007-9

[10] Li, G., Ma, X., Li, Z., & Li, Y. (2022). Optimal trajectory planning strategy for underactuated overhead crane with pendulum-sloshing dynamics and full-state constraints. *Nonlinear Dynamics*, *109*(2). https://doi.org/10.1007/s11071-022-07480-w

[11] Yu, Z., & Niu, W. (2023). Flatness-Based Backstepping Antisway Control of Underactuated Crane Systems under Wind Disturbance. *Electronics (Switzerland)*, *12*(1). https://doi.org/10.3390/electronics12010244

[12] Li, G., Ma, X., Li, Z., & Li, Y. bin. (2024). Trajectory Planning for Overhead Crane With Double Spherical Pendulum and Varying Cable Length Effect. *Zidonghua Xuebao/Acta Automatica Sinica*, *50*(5). https://doi.org/10.16383/j.aas.c220988

[13] Mustafa, A. M., Brahmi, B., & Iqbal, N. (2025). Optimised Integral-LQR Control and Crane-Adapted Dynamic Window Approach Algorithm for 3D Overhead Crane Path Planning. *ICAC 2025 - 30th International Conference on Automation and Computing*. https://doi.org/10.1109/ICAC65379.2025.11196637

[14] Yunsheng, X., Shuyi, L., Xinyu, Y., Ziyue, L., & Yueru, Y. (2025). MECHANICAL CHARACTERISATION OF TELESCOPIC BOOM HINGE POINT OF TRUCK CRANE BASED ON ADAMS. *International Journal of Mechatronics and Applied Mechanics*, *2025*(19). https://doi.org/10.17683/ijomam/issue19.10

[15] Perig, A. v., Stadnik, A. N., Kostikov, A. A., & Podlesny, S. v. (2017). Research into 2D Dynamics and Control of Small Oscillations of a Cross-Beam during Transportation by Two Overhead Cranes. *Shock and Vibration*, *2017*. https://doi.org/10.1155/2017/9605657

[16] Basova Y., Dobrotvorskiy S., Talar R. The Role of Digitalisation and 3D Information in the Technological Preparation of Manufacturing for Engineering Components in SMEs. International Conference on Reliable Systems Engineering (ICoRSE) - 2025. ICoRSE 2025. Lecture Notes in Networks and Systems. Vol. 1592. Springer, Cham, 2025. P. 229-239. https://doi.org/10.1007/978-3-032-02508-1_20

[17] Andrei, N. (2022). Sequential Quadratic Programming. In *Springer Optimization and Its Applications* (Vol. 195). https://doi.org/10.1007/978-3-031-08720-2_15